# Utilizing Helicoidal and Translational Symmetries Together in 2-D Models of Twisted Litz Wire Strand Bundles

Antero Marjamäki, Timo Tarhasaari, and Paavo Rasilo

Electrical Engineering Unit, Tampere University, 33720 Tampere, Finland

**In this article, a helicoidally symmetric 2-D model of a twisted litz wire strand bundle is studied. Suitable foundations for compatibility tools are presented to use such a model as a part of a larger system which does not follow a helicoidal symmetry. A measure for the symmetricity of a field is proposed. This provides the foundations for the coupling of helicoidally symmetric and translationally symmetric models with good understanding of the introduced approximation error.**

*Index Terms*—**Finite element method, helicoidal symmetry, litz wire, translational symmetry.**

## I. Introduction

INCREASING operating frequencies of power electronics requires using litz wires to keep eddy-current losses of windings at an acceptable level. Important applications for litz wires are, e.g., wireless power transfer coils [1] and windings in power electronic converters' magnetic components [2] and high-speed electrical machines [3].

Litz wires are made of thin electrically isolated strands of conducting material. Typically, there are hundreds or thousands of strands assembled in a bundled configuration. The strand bundles and bundles of bundles are usually twisted in a helicoidal shape to even out the proximity effects caused by the adjacent bundles or winding turns.

Windings made of litz wire are difficult to model due to their complex and fine-detailed multi-scale nature. However, detailed modeling of litz wires is crucial, as existing research suggests that choosing a suitable litz wire configuration is more complex than picking the strand diameter and the number of strands. It is reported in [3] that, e.g., the bundle configuration and shape of the strand have a significant impact on the total losses of litz wire windings in high-speed machines.

The computational burden of simulating the losses emerging in a device which includes litz wire windings is prohibitive without the application of special techniques. Because of this, the engineering field is constantly looking for new methods of incorporating litz wires more accurately in the computational models [4], [5], [6]. Symmetries of the modeled device, e.g., translational symmetry or rotational symmetry, are typically exploited to reduce the problem domain from 3-D to 2-D. If neither symmetry is directly applicable, the so-called multi-slice models can be used [7]. This reduction in dimension typically sacrifices some of the 3-D properties of the problem, one of which is the helicoidal twisting of the strands and bundles. To account for the twisting in an approximate manner, one needs to use multiple slices where the locations of the strands are varied from slice to slice.

Manuscript received 10 October 2022; revised 13 January 2023; accepted 13 January 2023. Date of publication 18 January 2023; date of current version 25 April 2023. Corresponding author: A. Marjamäki (e-mail: antero.marjamaki@tuni.fi).

Color versions of one or more figures in this article are available at https://doi.org/10.1109/TMAG.2023.3237767.

Digital Object Identifier 10.1109/TMAG.2023.3237767

In this article, a 2-D model for a twisted strand bundle is developed using helicoidal symmetry and dimensional reduction [8]. This method has been used successfully in computing self-fields of superconducting cables [9] and power cables [10], but there was no attempt to connect the helicoidally symmetric model to any larger system. The novelty of this article is in using the familiar concept of harmonic fields, commonly used to model time-periodic signals, to capture the twisting effects.

## II. Methods

A 2-D model of a litz wire with $n_{\mathrm{str}}$ parallel strands is considered. The wire is assumed to be helicoidal with a pitch length $l_z$. The computational domain is divided into three parts: the Cartesian domain $\Omega_c$, the twisting effects' domain $\Omega_{tw}$, and the helicoidal domain $\Omega_h$ (see Fig. 1). In a cross section of a litz wire, the strands are more distorted the further they are from the twisting axis. We use circular strand cross sections for simplicity. The 3-D geometry is extruded from the 2-D slice, and hence the 2-D geometry is an accurate representation of the 3-D geometry. The 3-D geometry, however, is only an approximation of a real litz wire structure.

Our aim is to keep $\Omega_{tw}$ as small as possible and free of conducting and nonlinear materials. In this article, we do not yet have the tools to incorporate $\Omega_c$ into the computational model. Hence, we consider the area $\Omega = \Omega_{tw} \cup \Omega_h$. Two charts are used to cover the domain: a Cartesian chart $\chi_c$ which covers the whole domain $\Omega_c \cup \Omega$ and a helicoidal chart $\chi_h$ which covers $\Omega$ (see Fig. 2). As the charts are overlapping in $\Omega$, a transition map $\chi = \chi_h^{-1} \circ \chi_c$ exists and we can change the representation of fields in $\Omega$ between the coordinate systems. It might be confusing that $\chi_c$ and $\chi_h$ are not explicitly stated. What we have is certain properties, such as material parameters, measured using $\chi_c$ and we want to represent them using $\chi_h$. That is why we only need to instantiate the transition map $\chi$ which defines the relationship between $\chi_c$ and $\chi_h$.

For brevity, let $c = \cos(\alpha w)$ and $s = \sin(\alpha w)$, where $\alpha = (2\pi / l_z)$. The transition map is

$$\chi : \begin{bmatrix} u \\ v \\ w \end{bmatrix} \mapsto \begin{bmatrix} x \\ y \\ z \end{bmatrix} = \begin{bmatrix} uc - vs \\ us + vc \\ w \end{bmatrix}. \tag{1}$$

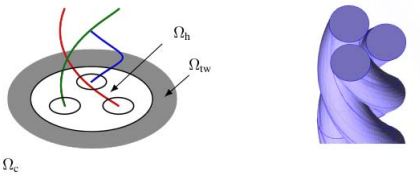


Fig. 1. 2-D slice of the helicoidal wire and an illustration of the 3-D geometry.

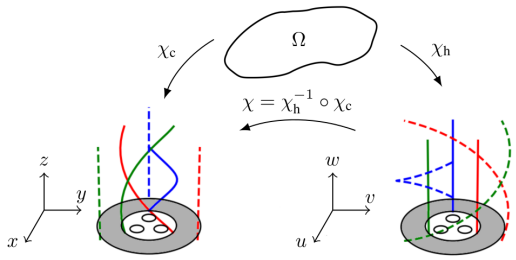


Fig. 2. Charts for Cartesian $\chi_c$, and helicoidal $\chi_h$ coordinates and the transition map $\chi$ from the helicoidal coordinate system $(u, v, w)$ into the Cartesian coordinate system $(x, y, z)$. Figure illustrates how the Cartesian chart $(x, y, z)$ and helicoidal chart $(u, v, w)$ see the $z$-directional coordinate fibers (dashed lines) and the $w$-directional coordinate fibers (solid lines) in the twisting effect region (gray area).

The Jacobian matrix of the transition map is

$$\mathrm{J}_\chi = \begin{bmatrix} c & -s & -\alpha(us + vc) \\ s & c & \alpha(uc - vs) \\ 0 & 0 & 1 \end{bmatrix}. \tag{2}$$

The magnetostatic problem is defined by the equations

$$\mathrm{d}H = J \tag{3}$$

$$\mathrm{d}B = 0 \tag{4}$$

$$H = \nu \star B \tag{5}$$

where d is the exterior derivative, $H$ is the magnetic field strength, $B$ is the magnetic flux density, $J$ is the current density, and $\nu$ is the reluctivity tensor. By representing the magnetostatic problem in the $(u, v, w)$ coordinates, we can reduce the problem into a 2-D translational symmetric problem. See [8] and [9] for a detailed description of the reduction. The difference compared with a Cartesian translational symmetric problem is visible in the material law

$$\begin{bmatrix} H_\mathrm{u} \\ H_\mathrm{v} \\ H_\mathrm{w} \end{bmatrix} = \nu_0 \begin{bmatrix} 1 & 0 & -\alpha v \\ 0 & 1 & \alpha u \\ -\alpha v & \alpha u & \Gamma \end{bmatrix} \begin{bmatrix} B_\mathrm{u} \\ B_\mathrm{v} \\ B_\mathrm{w} \end{bmatrix} \tag{6}$$

where $\Gamma = 1 + \alpha^2(u^2 + v^2)$.

The translational symmetric problem is formulated by having the out-of-plane components of the vector potential $A_\mathrm{w}$ and the magnetic field $H_\mathrm{w}$ as unknowns. Equations (3)–(5) then become

$$\begin{bmatrix} \partial_u & \partial_v \end{bmatrix} \left( \frac{\nu_0}{\Gamma} \begin{bmatrix} 1 + \alpha^2 v^2 & -\alpha^2 uv \\ -\alpha^2 uv & 1 + \alpha^2 u^2 \end{bmatrix} \begin{bmatrix} \partial_u A_\mathrm{w} \\ \partial_v A_\mathrm{w} \end{bmatrix} \right) - \frac{2\alpha}{\Gamma^2} H_\mathrm{w} = J_\mathrm{w}. \tag{7}$$

To solve $H_\mathrm{w}$, we need one more equation. It can be obtained by setting the average of the out-of-plane component of the magnetic flux density to zero

$$\int_\Omega B_\mathrm{w} \mathrm{d}u \wedge \mathrm{d}v = 0 \tag{8}$$

which leads to

$$\int_\Omega \left( \frac{\mu_0}{\Gamma} H_\mathrm{w} + \frac{\alpha}{\Gamma} (v \partial_v A_\mathrm{w} + u \partial_u A_\mathrm{w}) \right) \mathrm{d}u \wedge \mathrm{d}v = 0. \tag{9}$$

The system consisting of (7) and (9) is discretized with 2-D finite-element discretization and solved in the $w = 0$ plane.

## III. Symmetry of a Field

We interpret symmetry of a field as immutability of the field in the direction of the symmetry. Formally, as a measure for symmetricity we propose the Lie derivative of a field along the symmetry flow. For example, the Cartesian translational symmetry flow is expressed using a vector field $Z$, such that it defines the $z$-direction at every point in the domain. The vector field $Z$ is part of the $xyz$-coordinate frame. It acts as a directional derivative for the coordinate 0-forms $x$, $y$, and $z$ such that $Z(x) = Z(y) = 0$, and $Z(z) = 1$. The Lie derivative of any $p$-form $\eta$ with respect to vector field $Z$ can be calculated using Cartan's magic formula

$$\mathcal{L}_Z \eta = \mathrm{d} i_Z \eta + i_Z \mathrm{d}\eta \tag{10}$$

where $i_Z$ is the contraction along the vector field $Z$. The contraction is linear with respect to its vector field argument, and hence $i_Z$ can be expressed in the $uvw$-coordinates as

$$i_Z = \frac{\partial u}{\partial z} i_U + \frac{\partial v}{\partial z} i_V + \frac{\partial w}{\partial z} i_W = -\alpha v i_U + \alpha u i_V + i_W \tag{11}$$

where $U$, $V$, and $W$ are the vector fields along the coordinate axes of the helicoidal $uvw$ coordinate system. Note that because $z = w$ in the transition map, $dz = dw$ holds, but $Z = W$ does not.

The expression for the Lie derivative of a helicoidally symmetric $H$ can be derived to be

$$\begin{aligned} \mathcal{L}_Z H = {} & (-\alpha v \partial_u H_\mathrm{u} + \alpha H_\mathrm{v} + \alpha u \partial_v H_\mathrm{u}) \mathrm{d}u \\ & + (-\alpha H_\mathrm{u} + \alpha u \partial_v H_\mathrm{v} - \alpha v \partial_u H_\mathrm{v}) \mathrm{d}v \\ & + (-\alpha v \partial_u H_\mathrm{v} + \alpha u \partial_v H_\mathrm{u}) \mathrm{d}w. \end{aligned} \tag{12}$$

In (12), we have used the fact following from our interpretation of symmetry that for a helicoidally symmetric $H$, the partial derivatives with respect to coordinate $w$ of its component functions are $\partial_w H_\mathrm{u} = \partial_w H_\mathrm{v} = \partial_w H_\mathrm{w} = 0$.

Based on our interpretation of symmetry, the field $H$ is symmetric with respect to a vector field $Z$ if

$$\mathcal{L}_Z H = 0. \tag{13}$$

Our hypothesis is that the field $H$, emerging from the helicoidally twisted wire, can be considered $z$-symmetric when $\mathcal{L}_Z H$ becomes negligible. If the pointwise norm of the Lie derivative $||\mathcal{L}_Z H||$ is small enough around a point, $H$ can be considered translationally symmetric, with respect to $Z$, around that point. Fig. 3 visualizes how the symmetricity of the field varies. The norm has the highest values close to the bundle, and the value decays with respect to the distance from the bundle.

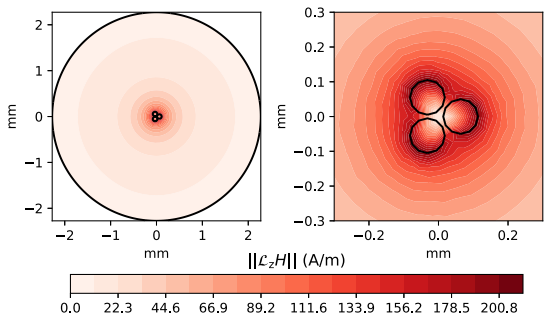


Fig. 3. Behavior of $||\mathcal{L}_Z H||$ in the $xy$-plane. The strand diameter is 0.1 mm, and the pitch length $l_z = 35$ mm.

The decay does not happen quickly enough to justify neglecting the twisting effects right outside the bundle. In a winding made of twisted litz wires the bundles are packed close to each other, and thus the twisting effects penetrate the neighboring bundles and any, possibly magnetic, nonlinear and conducting, materials close to the windings. Therefore, by simplifying a litz bundle to be translationally symmetric with respect to the $z$-coordinate, we introduce error to the computational model.

## IV. Multiharmonic Fields

Since bundle twisting effects on the magnetic field distribution cannot be neglected, we need a way to incorporate them to the Cartesian translational symmetric model in $\Omega_c$. We would like to express a helicoidally symmetric field with something that is more compatible with the $z$-symmetry. As helicoidally symmetric fields are periodic with respect to the $z$-coordinate, they can be expressed using a Fourier series. We are interested in how well such fields can be approximated using a finite number of harmonics, i.e., what we call $z$-multiharmonic fields.

Analogously to the multiharmonic models in the time domain [11], we say that the field $H$ is $z$-multiharmonic if there exist complex valued 1-forms $\hat{H}_k$ such that

$$H(x, y, z) = \mathrm{Re}\left\{ \sum_{k=-K}^{K} \hat{H}_k(x, y) e^{j\alpha k z} \right\}. \tag{14}$$

To compute the coefficients $\hat{H}_k$, the representation of the helicoidally symmetric $H$, obtained in the $uvw$-coordinates, must be changed. We can change the representation of $H$, inside $\Omega_{\mathrm{tw}}$, with the help of the Jacobian as

$$\begin{bmatrix} H_{\mathrm{x}} \\ H_{\mathrm{y}} \\ H_{\mathrm{z}} \end{bmatrix} = \mathrm{J}_{\chi}^{\mathrm{T}} \begin{bmatrix} H_{\mathrm{u}} \\ H_{\mathrm{v}} \\ H_{\mathrm{w}} \end{bmatrix}. \tag{15}$$

The coefficients $\hat{H}_{\mathrm{x},k}$, $\hat{H}_{\mathrm{y},k}$, and $\hat{H}_{\mathrm{z},k}$ can then be calculated as integrals over one period of length $l_z$ along the $z$-directional fiber of the Cartesian coordinate system

$$\hat{H}_{i,k}(x, y) = \frac{1}{l_z} \int_{-l_z/2}^{l_z/2} H_i(x, y, z) e^{-j\alpha k z} \mathrm{d}z \tag{16}$$

where $i \in \{x, y, z\}$. Since the solution is helicoidally symmetric, the values of the field on a $z$-directional line are equivalent to values of the field in a circle around the bundle on the $xy$-plane. Hence, the coefficients can be computed from the information available in the 2-D helicoidally symmetric model.

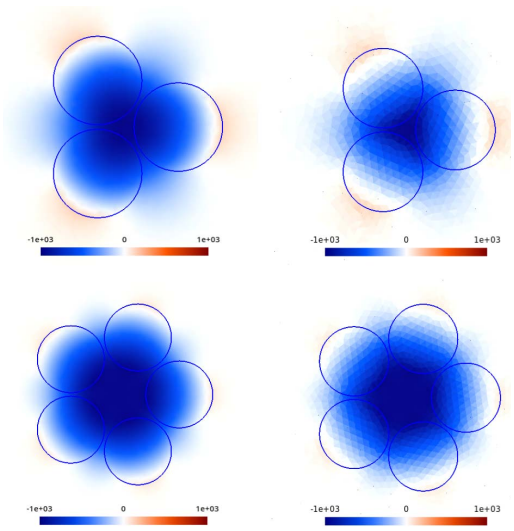


Fig. 4. Comparison of the $H_z$ component (in A/m) from the 2-D model using helicoidal symmetry (left side) and a 3-D model (right side) with three and five strands. The $H_z$ component is completely neglected in simplified translational symmetric 2-D models.

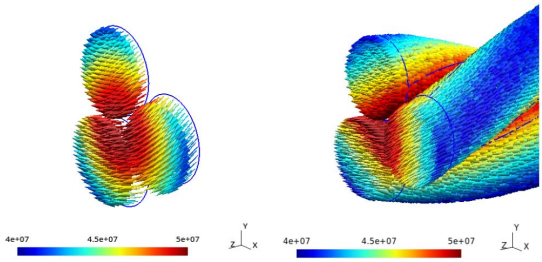


Fig. 5. Comparison of the current density proxy vector fields (in A/m$^2$) of the 2-D and 3-D models.

## V. Results and Discussion

Wires with three and five copper strands of diameter 0.1 mm, of pitch length 1 mm, and of net current 1 A were simulated using the 2-D symmetric model and a full 3-D model. The parts outside the strands are considered as air. In Fig. 4, the $z$-component of the magnetic field is shown. The field is the strongest in the middle and decays rapidly outside the bundle. This component of $H$ is neglected entirely in a Cartesian translationally symmetric 2-D model. In Fig. 5, the current density in the strands is shown. It is worth to note that as a simplification in the 2-D model, $J$ is forced to be parallel to the helicoidal strands. In the 3-D model used for comparison, this restriction is not present. The 3-D model was exited by a voltage source $V_{\mathrm{in}}$, whereas the 2-D model was exited by an equivalent $w$-directional electric field $E_{\mathrm{in}} = (V_{\mathrm{in}}/l_z)$. Both the inputs resulted in a net current of 1 A in the wire. The results between the 2-D and 3-D models match well, which corresponds to the observations made in [9].

Next, the harmonic components of the magnetic field were computed with $n_{\mathrm{str}} = 2, 3, \ldots, 9$ copper strands in the bundle. The strand diameter, pitch length, and net current are 0.1 mm, 35 mm, and 1 A, respectively. Fig. 6 visualizes the harmonic components $\hat{H}_k$ of $H$ for the case $n_{\mathrm{str}} = 3$. We observed that

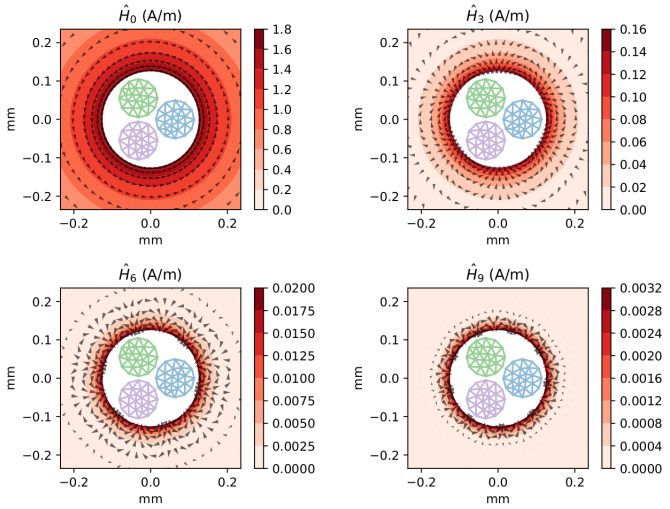


Fig. 6. Four biggest harmonic components of $H$ by magnitude in the $xy$-plane in the case of three strands. The colormap shows the norm $||\hat{H}_k||$, and the quiver shows the real part $\mathrm{Re}\{\hat{H}_k\}$ of the component field.

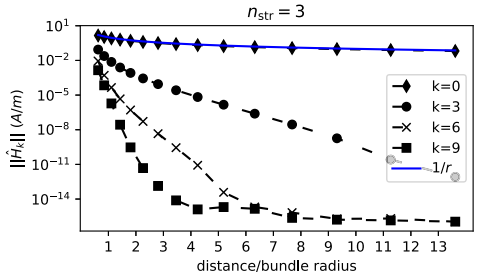


Fig. 7. Behavior of the four biggest harmonic components of $H$ by magnitude, with respect to the distance from the center of the bundle in the case of three strands.

the four most significant harmonic components, in descending order by magnitude, are $k = 0$, $k = n_{\mathrm{str}}$, $k = 2n_{\mathrm{str}}$, and $k = 3n_{\mathrm{str}}$. The $k = 0$ component is analogous to a dc-offset in a time-multiharmonic signal. It is the component of the helicoidally symmetric $H$ which already is $z$-symmetric. The components $k > 0$ correspond to the nonsymmetric parts which would be completely neglected in a translationally symmetric model. From Fig. 7, it can be seen more precisely how the different harmonic components behave with respect to the distance from the center of the bundle. The $k = 0$ harmonic decays inversely proportional to the distance, as is expected based on the Biot–Savart law. The $k > 0$ components decay more rapidly. This matches our intuition that one cannot differentiate a twisted and an untwisted wire bundle if they are observed at distance.

## VI. Conclusion

The behavior of the twisting effects of a litz wire bundle was studied, using a helicoidally symmetric 2-D model. In this article, the harmonic components are computed in a postprocessing phase, so the coupling between the Cartesian translational symmetry and helicoidal symmetry is only unidirectional. A bidirectional coupling is required to fully use the approach. It is our hypothesis that any helicoidally symmetric field in $\Omega_{\mathrm{h}} \cup \Omega_{\mathrm{tw}}$ can be represented as a $z$-multiharmonic field in $\Omega_{\mathrm{c}}$, and any $z$-symmetric field in $\Omega_{\mathrm{c}} \cup \Omega_{\mathrm{tw}}$ can be represented as a $w$-multiharmonic field in $\Omega_{\mathrm{h}}$. Then, by introducing suitable coupling conditions in $\Omega_{\mathrm{tw}}$, we can leave the harmonic coefficients as unknowns and solve them from a single equation system. The tools and observations presented in this article serve as a foundation for future research on this topic.

## Acknowledgment

This work was supported in part by the European Research Council (ERC) under the European Union's Horizon 2020 Research and Innovation Programme under Grant Agreement 848590 and in part by the Academy of Finland under Grant 326485 and Grant 346440.

## References

[1] D. Barth, B. Klaus, and T. Leibfried, "Litz wire design for wireless power transfer in electric vehicles," in *Proc. IEEE WPTC*, May 2017, pp. 1–4.

[2] M. Kharezy, M. Eslamian, and T. Thiringer, "Estimation of the winding losses of medium frequency transformers with Litz wire using an equivalent permeability and conductivity method," in *Proc. EPE ECCE Europe*, Sep. 2020, pp. 1–7.

[3] M. S. C. Pechlivanidou and A. G. Kladas, "Litz wire strand shape impact analysis on AC losses of high-speed permanent magnet synchronous motors," in *Proc. WEMDCD*, Apr. 2021, pp. 95–100.

[4] J. Lyu, H. C. Chen, Y. Zhang, Y. Du, and Q. S. Cheng, "Litz wire and uninsulated twisted wire assessment using a multilevel PEEC method," *IEEE Trans. Power Electron.*, vol. 37, no. 2, pp. 2372–2381, Feb. 2022.

[5] A. Rosskopf and C. Brunner, "Enhancing Litz wire power loss calculations by combining a sparse strand element equivalent circuit method with a Voronoi-based geometry model," *IEEE Trans. Power Electron.*, vol. 37, no. 9, pp. 11450–11456, Sep. 2022.

[6] S. Ehrlich, H. Rossmanith, M. Sauer, C. Joffe, and M. Marz, "Fast numerical power loss calculation for high-frequency Litz wires," *IEEE Trans. Power Electron.*, vol. 36, no. 2, pp. 2018–2032, Feb. 2021.

[7] J. Panchal, A. Lehikoinen, and P. Rasilo, "Efficient finite element modelling of Litz wires in toroidal inductors," *IET Power Electron.*, vol. 14, no. 6, pp. 2610–2619, 2021.

[8] B. Auchmann, B. Flemisch, and S. Kurz, "A discrete 2-D formulation for 3-D field problems with continuous symmetry," *IEEE Trans. Magn.*, vol. 46, no. 8, pp. 3508–3511, Aug. 2010.

[9] A. Stenvall, T. Tarhasaari, F. Grilli, P. Raumonen, M. Vojenciak, and M. Pellikka, "Manifolds in electromagnetism and superconductor modelling: Using their properties to model critical current of twisted conductors in self-field with 2-D model," *Cryogenics*, vol. 53, pp. 135–141, Jan. 2013.

[10] A. Piwonski, J. Dular, R. S. Rezende, and R. Schuhmann, "2D eddy current boundary value problems for power cables with helicoidal symmetry," *IEEE Trans. Magn.*, early access, Jan. 4, 2023, doi: 10.1109/TMAG.2022.3231054.

[11] J. Gyselinck, P. Dular, C. Geuzaine, and W. Legros, "Harmonic-balance finite-element modeling of electromagnetic devices: A novel approach," *IEEE Trans. Magn.*, vol. 38, no. 2, pp. 521–524, Mar. 2002.